



Augmenting the Thermal Efficiency of Solar Stills Using Phase Change Material on a Rotating Hollow Cylinder

Suzan Abdulrhman Hameed^{1,2*}, Hussein Hayder Mohammed Ali^{1,2}, Shahren Mohammed Fakhraldin^{1,2}

¹ Kirkuk Technical Engineering College, Northern Technical University, Kirkuk 36001, Iraq

² Renewable Energy Research Center Kirkuk, Northern Technical University, Kirkuk 36001, Iraq

Corresponding Author Email: suzan.abdulrahman24gs@ntu.edu.iq

Copyright: ©2025 The authors. This article is published by IETA and is licensed under the CC BY 4.0 license (<http://creativecommons.org/licenses/by/4.0/>).

<https://doi.org/10.18280/ijht.430336>

ABSTRACT

Received: 20 April 2025

Revised: 28 May 2025

Accepted: 12 June 2025

Available online: 30 June 2025

Keywords:

thermal energy storage, phase change materials (PCMs), solar still, revolving hollow metal cylinder, double-tilt solar still

This study presents an experimental investigation into enhancing solar water desalination using phase change materials (PCMs) and geometric modifications in a double-slope solar still. Paraffin wax was employed as a thermal energy storage medium, encapsulated in copper tubes mounted on a revolving hollow metal cylinder to simulate the climate of Kirkuk, Iraq. The system was designed to increase the surface area of the basin water through a thin water film inside the rotating cylinder and to utilize the stored thermal energy during off-sunshine hours, thereby sustaining water evaporation and enhancing distillate output. Results showed a marked improvement in productivity: while the conventional solar still produced 410 mL/day in December 2024, the enhanced still operating at 0.25 rpm achieved a yield of 3400 mL/day. These findings demonstrate that integrating PCM with mechanical rotation significantly improves the performance of solar desalination systems, offering a sustainable solution for freshwater generation in arid regions.

1. INTRODUCTION

Water scarcity affects millions of people worldwide and continues to worsen due to a combination of factors, including rapid population growth, climate change, and poor water resource management [1-3]. According to the United Nations World Water Development Report, approximately 2 billion people—representing 26% of the global population lack access to safely managed drinking water services [4, 5]. Water pollution is also a major global health concern, as many infectious diseases are transmitted through contaminated water. This makes the provision of permanent and safe drinking water especially critical in remote and arid regions [6].

One key indicator of water quality is the Total Dissolved Solids (TDS) level; drinking water is considered acceptable when its TDS concentration remains below 500 mg/L [7, 8]. Addressing water scarcity and contamination requires sustainable solutions, and renewable energy plays a vital role in this effort. Harnessing clean energy sources—such as solar, wind, ocean, and geothermal helps reduce dependence on fossil fuels and mitigates environmental degradation. Among these, solar energy stands out as a promising and increasingly accessible resource. With advancements in photovoltaic technology and its ability to generate power even in off-grid areas, solar energy is poised to play a transformative role in both energy and water security. Elamy et al. [9] explored a series of enhancements to tubular solar stills to significantly boost freshwater production. By integrating wick cords, baffles, reflectors, and nanoparticle-enhanced phase change materials (nano-PCM), their modified system (CWTSS)

achieved up to a 256% increase in yield compared to a conventional still. The use of reflectors alone improved output by 201%, while nano-PCM integration led to a 240% gain. The most efficient setup, which combined a fan and external condenser, produced 15,300 mL/m²/day versus 4,300 mL/m²/day in the baseline design. Additionally, the cost of freshwater was halved to \$0.01/L, confirming the design's economic and thermal advantages. Its utility is most apparent in arid regions and other outlying areas. Solar water purification is an efficient process that uses solar energy to purify saline water so it can be used. There is hope that desalination systems powered by renewable energy can help alleviate water scarcity and pollution. Considered a key factor influencing. The production of freshwater in a solar still depends on the exposed surface area available for both condensation and evaporation processes. Mohamad [10] experimentally and numerically investigated heat transfer in a straight channel using Al₂O₃-water nanofluids with volume fractions of 1-3% and Reynolds numbers from 100 to 1800. A 3% concentration yielded a 53.8% increase in heat transfer, with minimal impact on friction. Simulation results closely matched experimental data, confirming the nanofluid's effectiveness. Solar distillers have been designed and modified in many ways to increase their evaporative surface area and, by extension, their production. Zarda et al. [11] numerically investigated the thermal performance of a flat plate solar collector (FPSC) using diamond/water nanofluids under Iraq's hot climate conditions. Simulations conducted with ANSYS/FLUENT showed that a 1% nanofluid concentration achieved the highest thermal efficiency of 68.9%, representing a 12.2% improvement over pure water. The enhanced

performance was attributed to improved thermal conductivity and physical properties of the nanofluid. The study also highlighted the direct correlation between solar radiation intensity and collector efficiency, peaking around 12:30 pm. Essa [12] conducted a study combining experimental and empirical methods to enhance the efficiency of tubular distillers using a dual-ended rotating drum. By incorporating an open-ended drum and a wick to expand the evaporative surface area, the system achieved a 170% increase in efficiency at a rotational speed of 0.05 rpm. Solar distillers equipped with mechanical components were proposed as a method to attain that objective. The kinetic components induce the water molecules at the surface to disrupt their bonds (interfacial tension) [13-16].

Khalaf et al. [17] reviewed recent innovations in solar still technologies, focusing on advanced materials, thermal management, and hybrid systems to enhance freshwater productivity and cost-efficiency. The study highlights significant gains using phase change materials (PCMs) (up to 140%) and thermoelectric modules (up to 6.7-fold). Integrated systems with nanofluids, fins, and external condensers demonstrated cost-effective water production, reaching as low as 0.011 USD/L. The review offers a comparative assessment of designs and emphasizes future potential in combining PCM, TEM, and nanotechnology for improved solar desalination. To improve the performance of solar stills, a spinning device called a rotating cylinder is utilized. Drum spinning speed, basin water depth, and cover cooling are three of the many factors that affect the efficiency of drum solar stills, and Ayoub et al. [18] examined all of these factors. Based on their research, it was found that the optimal speed for the drum is kept at a minimum to avoid dry areas on its surface and maximize its performance. Malaeb et al. [19] have suggested a solar distiller with a revolving cylinder to increase evaporative surface area and decrease salt water thickness. The freshwater productivity of the solar still was enhanced by 250% with this modification. The solar still developed by Abdullah et al. [20] featured a drum that could spin. They tested drum solar stills with different operational parameters, including condenser, solar air heater, nanofluid, and drum speed. Their claims for the traditional distiller were 2025 mL/m²/day, and for the drum distiller, they were 6420 mL/m²/day. The use of a spinning drum increased freshwater output by 217%. PCMs facilitate latent thermal energy storage by absorbing and releasing heat under controlled conditions without significant temperature variation. One of their key applications in solar stills is minimizing heat loss during peak solar radiation by storing thermal energy and releasing it during non-sunlight hours, such as at night. PCMs offer several advantages, including high storage capacity, low temperature fluctuation, congruent melting behavior, and noncorrosive properties. During periods without solar radiation, the stored thermal energy in the PCM is released, causing water in the basin to evaporate and thereby enhancing distillate production [21-24]. Furthermore, the efficiency gains from incorporating nanoparticles into PCMs depend on the type of nanoparticles, the specific PCM used, and the design of the solar still system. Elsheikh et al. [25] presented a comprehensive review of recent advancements in solar still (SS) performance enhancement techniques aimed at increasing freshwater productivity and supporting sustainable development goals. The study evaluated various methods including thermal energy storage, cooling strategies, water stirring, spraying, forced vibration, solar collectors, reflectors,

condensers, and multi-stage designs. It also covered emerging configurations such as floating and multiple-effect solar stills. Additionally, the review analyzed performance from thermal, economic, and life cycle perspectives. The authors concluded by identifying existing limitations and outlining future research directions for developing more efficient and sustainable solar desalination systems. An empirical analysis carried out by Alqsair et al. [26] aimed to enhance the efficiency of a rotary still by employing translucent panels, nanoparticle coatings, PCMs, a parabolic reflector, and an external condenser. A parabolic solar collector was employed to concentrate sunlight on the rear of the drum, hence enhancing the vaporization rate, and indicated that the highest production enhancement of 320% was achieved using a drum still featuring nano-coating, a parabolic dish concentrator, and a condenser. Mohammed et al. [27] provided an in-depth review of advancements in active solar stills integrated with solar concentrating systems for seawater desalination. The study highlights the growing importance of solar-powered desalination as a sustainable solution to the global freshwater shortage. It categorizes solar stills into active and passive types, emphasizing the role of external heat sources in active systems. The article examines various performance enhancement techniques aimed at improving water productivity, thermal efficiency, and overall output. The review serves as a valuable resource for researchers by summarizing key developments and future directions in the field of active solar desalination technologies.

The aim of this work is to enhance the thermal efficiency of solar stills by using phase change material applied to a rotating hollow cylinder. The experiments were conducted under the winter and spring conditions of Kirkuk city-Iraq.

2. EXPERIMENTAL METHODOLOGIES

Figures 1 and 2 illustrate the two main types of solar stills: traditional and modified designs. In the conventional solar still (Figure 1), a horizontal trough made of 0.05-meter-thick insulated glass is used. The basin has dimensions of 1.32 meters in length, 0.78 meters in width, and 0.15 meters in depth, resulting in a total surface area of one square meter. The basin is constructed from galvanized steel and painted opaque black to maximize solar radiation absorption. A glass cover, 0.004 meters thick, is mounted at an inclination angle ranging from 9° to 32° relative to the horizontal. The glass cover is installed over a vertical glass wall, with a rubber gasket applied to ensure a secure and sealed fit. A collection tube is firmly attached at the base of the basin to facilitate the collection of distilled water. Temperature measurements are taken on both the inner and outer surfaces of the glass cover. In contrast, the modified solar still (Figure 2) features an insulated container similar in dimensions to the conventional model, but incorporates a rotating hollow cylinder partially immersed in water. This rotating component enhances heat transfer and evaporation efficiency, offering improved thermal performance over the traditional configuration.

To enhance the manufacturing efficiency of the rotating hollow cylinder, PCM, specifically paraffin wax, is first melted and poured into copper tubes, as the thermophysical properties illustrated in Table 1. To prevent the wax from solidifying during the filling process, the section of the cylinder holding the tubes is placed in boiling water. Once filled, the tube openings are soldered shut to prevent leakage.

As shown in Figure 2, temperature gauges are strategically positioned on the upgraded solar panel for improved performance monitoring.

Table 1. Thermophysical properties of paraffin wax

Property	Value
The latent heat of melting	190 kJ/kg °C
Liquefaction point	55°C
Thermal transferability	0.19 W/m°C
Specific heat capacity	2.1 kJ/kg °C
Heat capacity ratio	870 kg/m ³
Fluid density	791 kg/m ³

2.1 Tools used in the experiment

2.1.1 The photovoltaic module

The photovoltaic (PV) system used in this study has dimensions of 1.48 meters in length, 0.68 meters in width, and 0.035 meters in height. It is capable of supporting electrical loads up to 150 W and generates 17.3 Ah of direct current (DC) power. Its primary role is to supply energy to the charge controller, which in turn powers the DC motor and other system components. To optimize solar energy capture, the PV panel is installed at a tilt angle of 32 degrees. Structurally, the panel is mounted on a frame made of four aluminum rods arranged in a rectangular configuration and secured with screws at measured intervals of 0.68 m and 1.48 m. A stationary pedestal provides the base support, while a movable pedestal allows the tilt angle to be adjusted as needed. The support structure also includes an umbrella-like assembly composed of four parts, with two aluminum pieces joined at right angles to match the dimensions of the stationary armrest, ensuring mechanical stability and optimal orientation toward the sun.

2.1.2 The solar charging controller

When using batteries in solar-powered systems, a solar charge controller is an essential component. Its primary function is to regulate the charging and discharging cycles of the batteries, thereby protecting them from overcharging and deep discharge both of which can significantly reduce battery lifespan. Once the batteries reach full charge, the charge controller automatically disconnects the power supply from the photovoltaic (PV) modules to prevent overcharging. It then restricts power flow until the battery voltage drops to a predefined threshold, at which point recharging resumes. Most modern charge controllers are designed to prevent full battery discharge, further extending battery life. In this system, the charge controller is mounted behind the solar panel for easy integration and maintenance.



(a) Conventional solar still



(b) Modified solar still

Figure 1. Solar still

For structural integration, eight copper tubes, each 16 mm in diameter and 1.5 meters in length are mounted around the outer surface of the hollow cylinder. These tubes are securely fastened using quick-release screws. Finally, both the cylinder and the copper tubes are coated with an opaque black paint to maximize solar energy absorption. This modification aims to improve the thermal performance and overall efficiency of the rotating hollow cylinder within the solar still system.

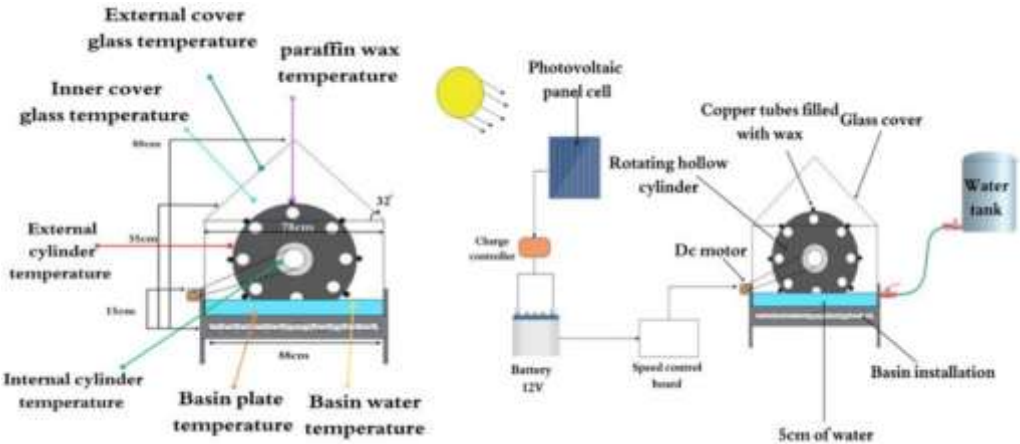


Figure 2. The description of the modified solar still

2.1.3 The battery

In situations where sunlight is not available, a 70 A heavy-duty calcium battery was used to power the DC motor's driving controller.

2.1.4 The DC motor

At the DC motor interface, a drive controller circuit is equipped with a variable-resistance volume switch to regulate motor operation. The system is powered by a photovoltaic panel and a battery managed through a charge controller, ensuring consistent energy supply. The DC motor, rated at 12 V with a torque output of 5.5 Nm and operating current range of 0.13-2.59 A, transmits rotational motion to the cylindrical component via a V-belt mechanism. This configuration enables controlled rotation of the hollow cylinder based on available solar energy.

2.1.5 Motor controller (DC)

A drive-controlled DC motor was used to regulate the rotational speed of the hollow cylinder based on real-time solar intensity. As sunlight intensity increases, the motor controller automatically raises the cylinder's rotational speed to enhance evaporation. Conversely, during periods of reduced solar radiation, the controller decreases the rotation rate to optimize energy use. This adaptive control is enabled by a built-in solar intensity sensor, which utilizes a Light Dependent Resistor (LDR) also known as a photoresistor.

An LDR is a light-sensitive, variable resistor that exhibits photoconductivity, meaning its resistance decreases as the intensity of incident light increases. Under strong sunlight, its resistance can drop to just a few ohms, while in low light, it can rise to over 1 megaohm. Due to their wavelength-dependent sensitivity, LDRs are classified as nonlinear devices. The LDR functions as part of an integrated circuit, generating a voltage signal that is directly proportional to solar intensity. This voltage input is processed by the drive controller to adjust the current and voltage supplied to the DC motor, effectively modifying its rotation speed.

The entire system is powered through a charge controller, which manages energy flow from the photovoltaic panel to ensure reliable operation of the motor and sensor circuitry without requiring external calibration.

2.1.6 Air velocity measurement

Model DA40 digital anemometers were used to measure air velocities. With a precision of 4%, the speed measurement spans from zero to forty meters per second.

2.1.7 The temperature measurement

Type-K thermocouples were employed to measure temperature at various points in the system. Each thermocouple was connected to a digital temperature reader (TES-1310A) via a selector switch, allowing accurate and sequential monitoring of temperature variations throughout the solar still components. This setup ensured reliable data acquisition for evaluating thermal performance.

3. ANALYTICAL MODEL

3.1 The hourly effectiveness of the solar stills

3.1.1 The hourly efficacy of traditional sun stills

The hourly operational efficiency of the conventional solar

still (η_h) was calculated based on the energy balance between the thermal energy input and the useful energy output. Specifically, the accumulated hourly distillate yield (m_{ewc}) was multiplied by the mean latent heat of vaporization (h_{fg}), which corresponds to the average basin water temperature (T_{wb} in °C). This thermal output was then divided by the product of the hourly solar radiation intensity $I(t)$ (in W/m²), the surface area of the basin ($A=1$ m²), and the time interval Δt (3600 seconds) to determine the efficiency. This approach provides a measure of how effectively the solar still converts incident solar energy into distilled water during each hour of operation.

$$\eta_{hc} = \frac{m_{ewc} * h_{fg}}{I(t) * A_{bp} * \Delta t} * 100\% \quad (1)$$

where, the cumulative hourly output of distilled water, m_{ewc} , for the conventional solar still in (kg/m² .hr), A_{bp} is the surface area of the basin plate (1 m²) and h_{fg} is average heat of transformation in (J/kg) is obtained by [28, 29]:

$$h_{fg} = 10^3 [25019 - 2.40706 \times T_{wb1} + 1.192217 \times 10^{-3} \times T_{wb}^2 - 1.5863 \times 10^{-5} \times T_{bw}^3] \quad (2)$$

3.1.2 The daily efficacy of modifying solar stills

The hourly efficiency η_{hm} of the enhanced solar still was determined by multiplying the cumulative distilled water production (m_{ewc}) by the average latent heat (h_{fg}) at the mean basin water temperature (T_{wb}) in Kelvin. The resultant number was subsequently divided by the mean daily solar radiation $I(t)$ W/m² across the entire area A (1 m²) and time interval Δt (3600) for both the enhanced solar still and the motor power consumption P_{motor} (4 W).

$$\eta_{hm} = \frac{m_{ewc} * h_{fg}}{I(t) * A_{bp} * \Delta t + (P_m * \Delta t)} \times 100 \% \quad (3)$$

3.1.3 The daily efficiency of traditional sun stills

In order to determine the traditional solar still's daily efficiency, η_{dc} , the sum of the hourly efficiency was added and then divided by the total number of hours of effective distillate water production:

$$\eta_{dc} = \frac{\sum_{i=1}^n \eta_h \cdot c}{n} \quad (4)$$

3.2 The daily effectiveness of the improved solar still

A modified solar still's daily efficiency, represented as η_{dm} , was calculated by adding up the hourly efficiency and dividing it by the entire number of hours of effective distillate water generation theoretical:

$$\eta_{dm} = \frac{\sum \eta_h \cdot m}{n} \quad (5)$$

4. RESULTS AND DISCUSSION

This study investigates two solar distillation systems: a conventional passive solar still and a modified active solar still. The conventional system operates without any thermal enhancement components, relying solely on direct solar radiation. In contrast, the modified system incorporates a rotating hollow metal cylinder fitted with copper tubes filled

with paraffin wax, a PCM. These copper tubes absorb and store thermal energy during peak sunlight hours and gradually release it later in the day, which helps maintain elevated water temperatures in the basin. This thermal regulation increases the evaporation rate and significantly enhances freshwater productivity, particularly during periods of reduced solar radiation.

The experimental systems were tested under the climatic conditions of Kirkuk, Iraq, over a three-month period from December 2024 to February 2025. Multiple environmental and design parameters, including solar radiation, ambient temperature, wind speed, and glass cover temperature, were found to influence daily water production. The rotating cylinder, combined with the latent heat storage of PCM, extended thermal activity beyond daylight hours, thereby sustaining distillation even into the evening.

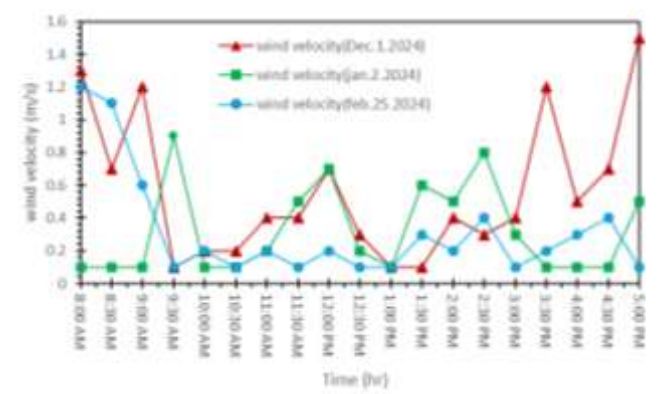


Figure 3. Relation between wind velocity and time for December, January, February, Kirkuk, Iraq

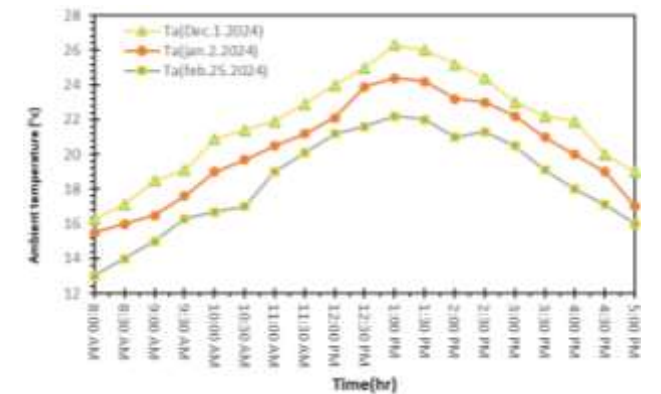


Figure 4. Correlation connecting time and ambient temperature for December, January, February, Kirkuk, Iraq

Environmental factors had a notable impact on system performance. As shown in Figure 3, air speed varied throughout the day across the three months, affecting the convective cooling of the glass cover and enhancing condensation efficiency. Figure 4 illustrates that February experienced generally higher ambient temperatures, likely due to increased sunlight duration and intensity. This greater solar exposure directly influenced the temperature of the basin water and the PCM, improving evaporation during daylight hours. Furthermore, Figure 5 demonstrates that December had the highest solar radiation intensity, which correlated with the highest water temperatures and evaporation rates. However, despite slightly lower radiation levels, February showed improved condensation efficiency due to cooler glass cover

temperatures and favorable wind conditions, contributing to higher overall thermal efficiency.

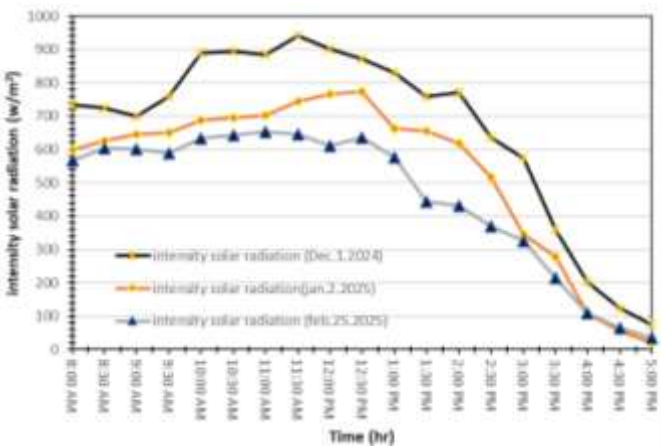


Figure 5. Relationship between sunlight intensity and time for December, January, February, Kirkuk, Iraq

Figures 6 and 7 illustrate the purified water output from both the conventional and modified solar stills during the months of December, January, and February. The data clearly indicate that the highest volume of distilled water was produced in December for both systems. This outcome is primarily attributed to the higher solar radiation intensity during December, which increased the basin water temperature and, consequently, the evaporation rate. As solar radiation is the driving force behind water evaporation in solar stills, greater sunlight exposure directly translates into higher water production. In contrast, the reduced solar intensity observed in January and February resulted in lower evaporation rates and, therefore, lower water yields. However, despite lower radiation, other environmental factors such as ambient temperature and wind speed influenced the overall system efficiency during these months.

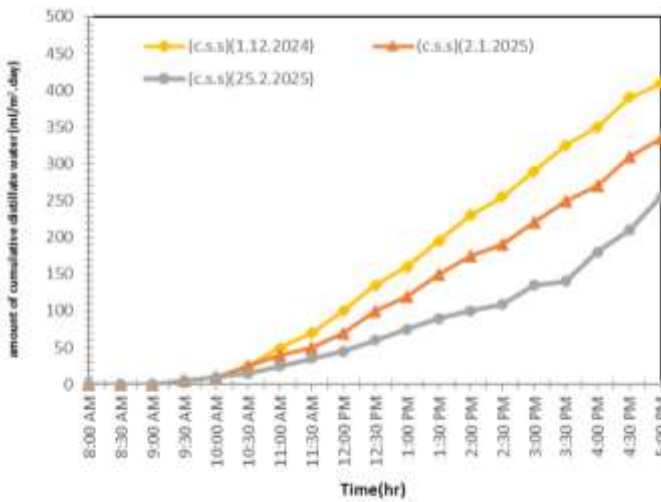


Figure 6. Relation between time and amount of cumulative distillate water for a conventional sun still at (5 cm depth of water) for different months

Figures 8 and 9 reveal that although December exhibited the highest distilled water production due to greater solar radiation, February demonstrated superior thermal efficiency. This apparent contradiction can be explained by considering the combined effects of solar input and condensation performance.

While February received slightly less solar radiation than December, the cooler ambient temperatures during this month significantly enhanced the condensation of water vapor on the inner surface of the glass cover. As condensation is a critical step in the distillation process, lower glass cover temperatures promote a higher condensation rate, thereby increasing the system's efficiency.

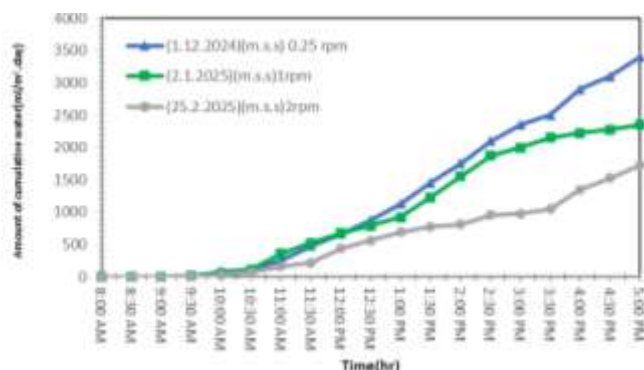


Figure 7. Association between time and cumulative water distillation for modified solar stills at 5 cm depth in Kirkuk, Iraq (December–February)

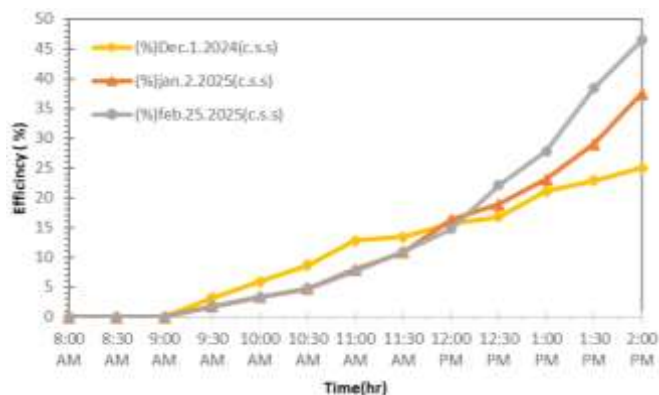


Figure 8. Association between time and the effectiveness of standard solar stills

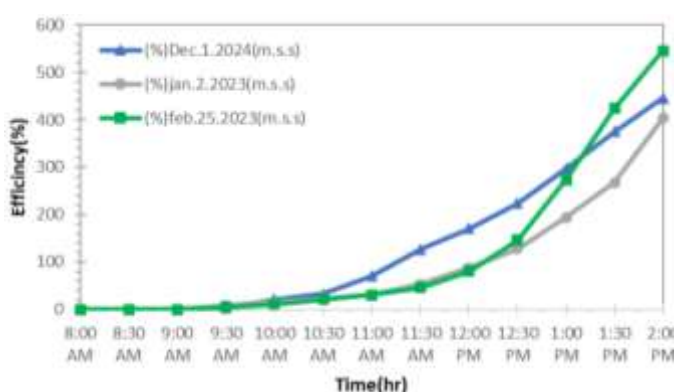


Figure 9. Connection between time and performance of upgraded solar stills across different months, 2025, Kirkuk, Iraq

It is important to note that thermal efficiency is not solely dependent on the volume of water produced but also on how effectively the available solar energy is converted into usable output. In February, although the evaporation rate was lower due to reduced solar intensity, the improved condensation

conditions resulted in more efficient utilization of the absorbed energy. This underscores the fact that efficiency is a function of both the quantity of distilled water generated and the ratio of useful thermal output to incoming solar radiation. Therefore, February's favorable ambient and thermal conditions contributed to a higher conversion efficiency, even with less total solar energy input compared to December.

Temperature measurements throughout the experiment were recorded using Type-K thermocouples, which were connected to a TES-1310A digital temperature reader and selector switch for precise monitoring. These thermocouples were used to continuously track the temperature of both the PCM, paraffin wax, and the basin water. As shown in Figure 10, the PCM and basin water temperatures exhibited a typical daily thermal cycle, rising steadily from the start of the experiment until midday, peaking around 1:30 PM when solar radiation was at its highest, and then gradually declining as solar intensity decreased.

The thermal charging process of the PCM can be divided into two distinct heating stages. In the first stage (Heating Process 1), the PCM absorbed convective heat transferred from the basin lining, causing its temperature to rise progressively. Once the PCM reached its melting point, between 30°C and 33°C around 11:00 AM, it began transitioning from solid to liquid. This melting process, due to the thin layer of PCM used, was rapid and completed within approximately 30 to 60 minutes. During this phase change, the temperature of the PCM plateaued, as the material absorbed latent heat without a significant rise in temperature.

Following complete melting at around 12:00 PM, the second stage of heating (Heating Process 2) began, driven by continued solar energy input. From 12:00 PM to 1:30 PM, the PCM temperature increased beyond that of the basin water, indicating that the PCM was actively storing additional sensible heat. This stored energy plays a crucial role in sustaining the evaporation process during periods of declining solar radiation.

After 1:30 PM, as solar intensity diminished and system heat losses increased, the PCM began the discharge phase. This phase included three stages: Cooling Stage 1, where the PCM temperature declined steadily; Solidification, during which the PCM released its latent heat and transitioned back to solid form (observed to occur between 3:00 PM and 4:00 PM); and Cooling Stage 2, where the PCM continued to cool down post-solidification. The effective heat storage and delayed energy release of the PCM contributed to sustained water evaporation in the later hours of the day, thus improving the overall productivity and efficiency of the solar still system.

During the solidification phase, the temperature of the PCM gradually decreases until it reaches its solidification point. As illustrated in Figure 10, between 3:00 PM and 4:00 PM, the temperature of the paraffin wax stabilizes, indicating the occurrence of a phase transition from the liquid to solid state. This thermal plateau reflects the release of latent heat as the PCM solidifies. The relatively thin layer of paraffin wax used in this setup enables the phase change to complete within approximately one hour, ensuring an efficient discharge of stored thermal energy back into the basin environment.

Following the completion of solidification at around 4:00 PM, the PCM continues to cool down in what is known as the post-solidification cooling phase. During this stage, the PCM, now fully solid, gradually releases residual sensible heat, contributing to the maintenance of a temperature gradient between the basin water and the cooler glass cover. This

gradient supports continued condensation of water vapor even as ambient and basin temperatures begin to decline. The effectiveness of this delayed heat release enhances the operational efficiency of the solar still by extending productive distillation hours beyond peak sunlight periods. This ability to sustain thermal activity during late afternoon hours is one of the key performance benefits of integrating PCM into the solar distillation system.

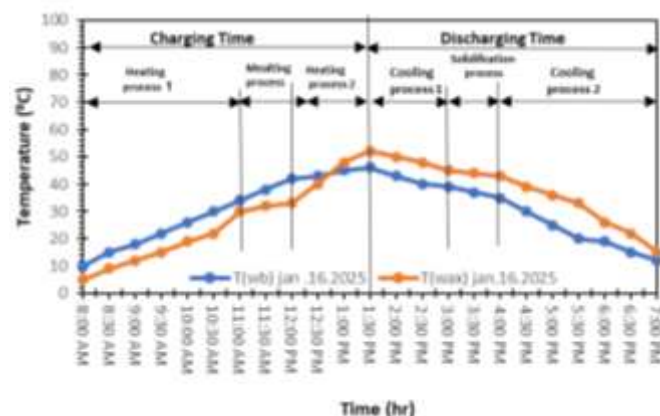


Figure 10. Relation between temperatures of basin water and PCM

The integration of a rotating hollow cylinder and copper tubes filled with PCM into the modified solar still significantly enhanced freshwater productivity from 410 mL/day in the conventional still to 3400 mL/day in the enhanced version during December 2024. While the modified system includes additional components such as a DC motor, photovoltaic panel, battery, and drive controller, the increased output justifies the added investment through improved cost-effectiveness over time.

Paraffin wax was selected due to its low cost, non-corrosive nature, stable thermal properties, and widespread availability. Similarly, the DC motor and drive system operate on low voltage (12 V) and minimal current, maintaining low operational power consumption (approximately 4 W), which is sustainably supplied by a small PV system. This off-grid design reduces dependency on external energy sources and minimizes long-term operational costs.

Considering the significant increase in daily water yield with only a modest rise in system complexity and energy input, the use of a rotating mechanism combined with PCM presents a cost-effective enhancement for solar distillation systems, especially in water-scarce, sun-rich regions like Kirkuk.

5. CONCLUSION

In this study, an experimental evaluation was conducted to assess the thermal performance and efficiency of a modified solar still integrated with a rotating hollow cylinder equipped with copper tubes filled with paraffin wax, a PCM. The system's productivity was benchmarked against that of a conventional passive solar still under the specific climatic conditions of Kirkuk, Iraq, during the winter and early spring months. The enhanced design aimed to improve heat retention and prolong the evaporation process through thermal energy storage and extended exposure surfaces. The key findings of the study are summarized as follows:

1. Solar radiation and ambient temperature play critical roles in influencing solar still performance. Higher solar intensity directly increases the basin water temperature, enhancing evaporation rates, while ambient temperature affects the condensation rate on the glass cover.
2. Wind speed was found to significantly aid in the condensation process. Airflow across the glass cover facilitates cooling, which improves the condensation of water vapor and subsequently increases the freshwater yield. This effect was particularly evident in February, when wind conditions supported higher efficiency despite lower solar intensity.
3. The study employed paraffin wax as the PCM due to its favorable thermal characteristics and economic advantages. Paraffin offers moderate thermal storage capacity, a stable and uniform melting point (around 30-33°C), good availability, safety, non-corrosiveness, and cost-effectiveness. These properties make it a suitable candidate for solar thermal energy storage applications.
4. The integration of copper tubes filled with paraffin wax onto the rotating cylinder significantly improved system performance. The rotating mechanism facilitated the formation of a thin water film on the cylinder's surface, increasing the evaporative area and promoting rapid heat transfer. The paraffin wax absorbed heat during peak solar hours and released it gradually during the evening, sustaining evaporation beyond sunlight hours.
5. As a result, the modified solar still demonstrated a substantial increase in freshwater output. For example, in December 2024, the conventional passive solar still produced only 410 mL of distilled water per day, whereas the enhanced still with the rotating PCM-filled cylinder yielded 3400 mL per day representing more than an eightfold increase in productivity. Future research should focus on optimizing the rotation speed of the hollow cylinder to maximize evaporation efficiency and adapt to varying solar conditions. Additionally, exploring alternative or nano-enhanced PCMs with higher thermal conductivity and energy density could further improve thermal performance. Studies on long-term durability, cost-effectiveness, and the integration of solar concentrators or multi-stage designs are also recommended to enhance practicality and scalability.

REFERENCES

- [1] Das, D., Bordoloi, U., Kalita, P., Boehm, R.F., Kamble, A.D. (2020). Solar still distillate enhancement techniques and recent developments. *Groundwater for Sustainable Development*, 10: 100360. <https://doi.org/10.1016/j.gsd.2020.100360>
- [2] Bayraktar, N., Abed, F.M., Ali, H.H.M. (2022). Design, simulation, construction of swimming pools: A comprehensive review. *NeuroQuantology*, 20(8): 8922. <https://doi.org/10.14704/nq.2022.20.8.NQ44914>
- [3] Ali, H.H.M., Hussein, A.M., Allami, K.M.H., Mohamad, B. (2023). Evaluation of shell and tube heat exchanger performance by using ZnO/water nanofluids. *Journal of Harbin Institute of Technology (New Series)*, 30: 1-13.
- [4] Najaf, F., Ridha, S. (2024). An analysis of the productivity of an active solar still vs. a passive solar still over the autumn and winter seasons in the city of Kirkuk, Iraq. *NTU Journal of Renewable Energy*, 6(1): 60-67.

- <https://doi.org/10.56286/4dhyse03>
- [5] Ali, H.H.M., Ahmed, S.Y. (2024). Assessing the economic viability of solar distillation employing a rotating hollow cylinder. *International Journal of Heat and Technology*, 42(2): 613-619. <https://doi.org/10.18280/ijht.420228>
 - [6] Yang, H.Y., Wang, Y., Liu, S.L., Tu, Q., Chen, G. (2024). Attenuation characteristics of ultrasonic waves from sonar logging tools in salt cavern gas storage. *Facta Universitatis, Series: Mechanical Engineering*, 22(4): 759-772. <https://doi.org/10.22190/FUME240118018Y>
 - [7] World Health Organization. (2011). *Guidelines for drinking-water quality* (4th ed.). WHO Chronicle.
 - [8] Barrak, A.S., Ali, N.M., Ali, H.H.M. (2022). An effect of binary fluid on the thermal performance of pulsation heat pipe. *International Journal of Applied Mechanics and Engineering*, 27(1): 21-34. <https://doi.org/10.2478/ijame-2022-0002>
 - [9] Elamy, M.I., Mohammed, S.A., Basem, A., Alawee, W.H., Aldabesh, A., Abdullah, A.S., Majdi, H.S., Omara, Z.M., Essa, F.A. (2024). Augmenting thermal performance in tubular solar stills: A multifaceted strategy with wick cords, integrated baffles, reflectors, and nano-PCM. *Results in Engineering*, 23: 102771. <https://doi.org/10.1016/j.rineng.2024.102771>
 - [10] Mohamad, B. (2025). Improving heat transfer performance of flat plate water solar collectors using nanofluids. *Journal of Harbin Institute of Technology (New Series)*, 32(2): 80-89. <https://doi.org/10.11916/j.issn.1005-9113.2024001>
 - [11] Zarda, F., Hussein, A., Danook, S., Mohamad, B. (2022). Enhancement of thermal efficiency of nanofluid flows in a flat solar collector using CFD. *Diagnostyka*, 23(4): 2022411. <https://doi.org/10.29354/diag/156384>
 - [12] A. Essa, F. (2022). Thermal desalination systems: From traditionality to modernity and development. In *Distillation Processes - From Solar and Membrane Distillation to Reactive Distillation Modelling, Simulation and Optimization*. <https://doi.org/10.5772/intechopen.101128>
 - [13] Alsehli, M., Essa, F.A., Omara, Z.M., Othman, M.M., Elsheikh, A.H., Alwetaishi, M., Alghamdi, S., Saleh, B. (2022). Improving the performance of a hybrid solar desalination system under various operating conditions. *Process Safety and Environmental Protection*, 162: 706-720. <https://doi.org/10.1016/j.psep.2022.04.044>
 - [14] Ahmed, S.T., Ali, H.H.M. (2020). Experimental investigation of new design of solar water distillation coupled with flat plate solar water collector. *The Iraqi Journal for Mechanical and Materials Engineering*, 20(3): 193-207. <https://doi.org/10.32852/ijqfmme.v20i3.512>
 - [15] Ali, H.H.M., Ahmed, S.Y. (2023). Exploring the enhancement of solar still performance through the utilization of solar water collectors, rotating hollow cylinders. *International Journal of Machine Tools and Maintenance Engineering*, 4(9). <https://doi.org/10.32852/ijqfmme.v20i3.512>
 - [16] Abbas, E.F., Ali, H.H.M., Mahmood, N.J. (2021). Comparison between numerical study and experimental work on heat transfer from heat sink under transient conditions. *Journal of Mechanical Engineering Research and Developments*, 44(7): 141-150.
 - [17] Khalaf, M.O., Özdemir, M.R., Sultan, H.S. (2025). A comprehensive review of solar still technologies and cost: Innovations in materials, design, and techniques for enhanced water desalination efficiency. *Water*, 17(10): 1515. <https://doi.org/10.3390/w17101515>
 - [18] Ayoub, G.M., Malaeb, L., Saikaly, P.E. (2013). Critical variables in the performance of a productivity-enhanced solar still. *Solar Energy*, 98: 472-484. <https://doi.org/10.1016/j.solener.2013.09.030>
 - [19] Malaeb, L., Aboughali, K., Ayoub, G.M. (2016). Modeling of a modified solar still system with enhanced productivity. *Solar Energy*, 125: 360-372. <https://doi.org/10.1016/j.solener.2015.12.025>
 - [20] Abdullah, A.S., Essa, F.A., Omara, Z.M., Rashid, Y., Hadj-Taieb, L., Abdelaziz, G.B., Kabeel, A.E. (2019). Rotating-drum solar still with enhanced evaporation and condensation techniques: Comprehensive study. *Energy Conversion and Management*, 199: 112024. <https://doi.org/10.1016/j.enconman.2019.112024>
 - [21] Abed, F., Ali, H.H.M., Bayraktar, N. (2023). Exploring the performance, simulation, design, and construction of a closed solar swimming pool in Kirkuk City. *Advances in Mechanical and Materials Engineering*, 40(1): 125-138. <https://doi.org/10.7862/rm.2023.13>
 - [22] Kabeel, A.E., Harby, K., Abdelgaied, M., Eisa, A. (2020). Augmentation of a developed tubular solar still productivity using hybrid storage medium and CPC: An experimental approach. *Journal of Energy Storage*, 28: 101203. <https://doi.org/10.1016/j.est.2020.101203>
 - [23] Vigneswaran, V.S., Kumaresan, G., Dinakar, B.V., Kamal, K.K., Velraj, R. (2019). Augmenting the productivity of solar still using multiple PCMs as heat energy storage. *Journal of Energy Storage*, 26: 101019. <https://doi.org/10.1016/j.est.2019.101019>
 - [24] Bazri, S., Badruddin, I.A., Naghavi, M.S., Bahiraei, M. (2018). A review of numerical studies on solar collectors integrated with latent heat storage systems employing fins or nanoparticles. *Renewable Energy*, 118: 761-778. <https://doi.org/10.1016/j.renene.2017.11.030>
 - [25] Elsheikh, A., Hammoodi, K.A., Ibrahim, A.M.M., Mourad, A.H.I., Fujii, M., Abd-Elaziem, W. (2024). Augmentation and evaluation of solar still performance: A comprehensive review. *Desalination*, 574: 117239. <https://doi.org/10.1016/j.desal.2023.117239>
 - [26] Alqsair, U.F., Abdullah, A.S., Omara, Z.M. (2022). Enhancement the productivity of drum solar still utilizing parabolic solar concentrator, phase change material and nanoparticles' coating. *Journal of Energy Storage*, 55: 105477. <https://doi.org/10.1016/j.est.2022.105477>
 - [27] Mohammed, A.H., Shmroukh, A.N., Ghazaly, N.M., Kabeel, A.E. (2023). Active solar still with solar concentrating systems: Review. *Journal of Thermal Analysis and Calorimetry*, 148: 8777-8792. <https://doi.org/10.1007/s10973-023-12285-z>
 - [28] Sahota, L., Tiwari, G.N. (2016). Effect of nanofluids on the performance of passive double slope solar still: A comparative study using characteristic curve. *Desalination*, 388: 9-21. <https://doi.org/10.1016/j.desal.2016.02.039>
 - [29] Abdullah, A.S., Essa, F.A., Ben Bacha, H., Omara, Z.M. (2020). Improving the trays solar still performance using reflectors and phase change material with nanoparticles. *Journal of Energy Storage*, 31: 101744. <https://doi.org/10.1016/j.est.2020.101744>